CrossMark

ORIGINAL ARTICLE

Reduced-dynamic and kinematic baseline determination for the Swarm mission

Gerardo Allende-Alba[1,2] · Oliver Montenbruck[1] · Adrian Jäggi[3] ·
Daniel Arnold[3] · Franz Zangerl[4]

Abstract The Swarm mission of the European Space Agency was launched in November 2013 with the objective of performing measurements of the earth's magnetic field with unprecedented accuracy. At the beginning of data collection, two satellites started to fly in orbits with a separation in ascending nodes of 1°–1.5° at an altitude of about 480 km, and a third satellite has been placed in a higher orbit with an altitude of 530 km. The three spacecraft are equipped with dual-frequency eight-channel GPS receivers for the generation of precise orbits. Although such orbits support the fulfillment of the primary objectives of the mission, precise space baselines may be helpful for studying the earth's gravity field, a spin-off application of the Swarm mission. Hitherto, a particular challenge for the computation of precise baselines from Swarm has been the presence of half-cycle ambiguities in GPS carrier phase observations, which complicate the implementation of integer ambiguity resolution methods. The present study shows the feasibility of generating carrier phase observations with full-cycle ambiguities, which in turn has been used to improve the performance of reduced-dynamic and kinematic precise baseline determination schemes. The implemented strategies have been tested in a period of 90 days in 2016. The obtained reduced-dynamic and kinematic baseline products were evaluated by inter-product and inter-agency comparisons using two independent software tools.

Keywords Swarm · Space baseline determination · Half-cycle ambiguity resolution · GPS

✉ Gerardo Allende-Alba
  gerardo.allendealba@dlr.de

  Oliver Montenbruck
  oliver.montenbruck@dlr.de

  Adrian Jäggi
  adrian.jaeggi@aiub.unibe.ch

  Daniel Arnold
  daniel.arnold@aiub.unibe.ch

  Franz Zangerl
  franz.zangerl@ruag.com

[1] Deutsches Zentrum für Luft- und Raumfahrt (DLR), German Space Operations Center (GSOC), 82230 Weßling, Germany

[2] Institute for Astronomical and Physical Geodesy, Technische Universität München, 80333 Munich, Germany

[3] Astronomical Institute, Universität Bern, 3012 Bern, Switzerland

[4] RUAG Space GmbH, 1120 Vienna, Austria

Introduction

The ESA's Swarm mission was successfully launched on November 22, 2013, with the fundamental goal of performing measurements with unprecedented accuracy for the study of earth's magnetic field (Friis-Christensen et al. 2006, 2008). The mission comprises three spacecraft called the Earth's Magnetic Field and Environment Explorers, commonly referred to as Swarm satellites A, B and C. The initial orbit configuration for data collection consists of two spacecraft with east–west separation of 1°–1.5° and at altitude of about 480 km and a third spacecraft at altitude of about 530 km. Starting from April 2014, the Swarm A and Swarm C were placed in the lower orbits, whereas Swarm B was left in the upper orbit (Mackenzie et al. 2014).

As a spin-off application of the Swarm constellation, data derived from the GPS receivers onboard the spacecraft can be used for the generation of geodetic products using

high–low satellite-to-satellite (hl-SST) data (Gerlach and Visser 2006). Further studies have effectively demonstrated the feasibility of using GPS data from each Swarm spacecraft for earth's gravity field determination (Jäggi et al. (2016); Teixeira da Encarnação et al. (2016) and references within). In this way, the Swarm mission will allow continued monitoring of the earth system for gravity field determination during an intermission gap between of the GRACE mission (Tapley et al. 2004) and the GRACE Follow-On mission, which is expected to be launched after August 2017 (Flechtner et al. 2014).

Unlike some past hl-SST missions (CHAMP, Reigber et al. 2002), the Swarm constellation offers, in addition, the possibility of baseline reconstruction, i.e., low–low satellite-to-satellite or ll-SST data. Such data can provide added information for the refinement of gravity models. Simulation-based studies have suggested that the use of single-satellite orbits in combination with baseline products can be used for the determination of the static field, offering an improved precision with respect to single-satellite-only solutions (Wang and Rummel 2012). Nevertheless, an in-depth analysis remains to be carried out, as pointed out by Jäggi et al. (2009a), exploring the actual potential benefit of precise kinematic baselines using real data for gravity field determination, now in particular for the Swarm mission.

The key for precise baseline determination (PBD) is the use of carrier phase measurements with fixed integer ambiguities. However, unlike other geodetic-class GPS receivers used in previous formation flying missions, such as GRACE and TanDEM-X (Krieger et al. 2010), the GPS receivers in the Swarm spacecraft generate carrier phase measurements also at half cycles in their default configuration. This fact necessitates the consideration of half-cycle ambiguities in the observation models, which complicates the implementation of integer ambiguity resolution (IAR) strategies. Jäggi et al. (2014) showed first the feasibility of computing precise baselines of Swarm A and Swarm C using fixed ambiguities based on the wide-lane/narrow-lane (WL/NL) approach, as described by Jäggi et al. (2007). Allende-Alba and Montenbruck (2016) and Mao et al. (2016) proposed tailored algorithms for ambiguity resolution on L1 and L2 for coping with the presence of half-cycle ambiguities. A further analysis performed by Jäggi et al. (2016) confirmed the possibility of ambiguity fixing and precise baseline reconstruction, and its possible use for gravity field determination.

Although the described algorithms have demonstrated that IAR can be performed even in the presence of half-cycle ambiguities, the lack of integer ambiguities influences the overall complexity of the algorithms and the capability of a successfully fixing. The present study introduces an alternative strategy to resolve the half-cycle ambiguity during the process of generation of carrier phase

observations from raw GPS data. Therefore, the generated observations are guaranteed to have integer-valued double-difference ambiguities, which allow executing IAR schemes without further special considerations or assumptions.

We start with a brief description of the GPS receivers on board the Swarm spacecraft and the process of half-cycle ambiguity resolution during the generation of carrier phase observations. Subsequently, the description is focused on the strategies for IAR and space baseline determination used in the present study, followed by a discussion of results obtained from actual flight data.

GPS receivers and carrier phase observations

For the generation of precise orbit determination (POD) products, each Swarm spacecraft is equipped with a high-end geodetic-type dual-frequency GPS receiver (called GPSR), manufactured by RUAG Space (Zangerl et al. 2014). The variant of the GPSR receiver onboard the Swarm spacecraft has eight channels and delivers dual-frequency measurements for the legacy signals. During the first months of operation, the three GPSR receivers provided measurements at a rate of 0.1 Hz, which was enough for the generation of POD products, also called precise science orbits (PSOs, van den IJssel et al. 2015). During this period, baseline determination was not possible due to lacking synchronization of the measurement epochs across the different spacecraft. However, on July 15, 2014, the receiver configuration was modified, and the observation-delivery rate changed to 1 Hz (Jäggi et al. 2014), hence offering the possibility of baseline reconstruction.

Signal tracking concepts

The GPSR instrument is based on the space-hardened AGGA-2 (Advanced GPS/GLONASS ASIC) correlator chip, which has been developed in an initiative of the European Space Agency (ESA). It is specifically designed to support semi-codeless tracking of the encrypted P(Y) signal on the L1 and L2 frequencies along with the direct tracking of the L1 C/A code. AGGA-2-based GPS receivers for radio occultation observations and POD have previously been flown on Metop (Silvestrin et al. 2000; Montenbruck et al. 2008), GOCE (Zin et al. 2006; Bock et al. 2011) as well as various other international missions. With a total of two AGGA-2 chips, the Swarm GPSR supports concurrent tracking of L1 C/A, L1 P(Y) and L2 P(Y) for up to eight satellites.

Following the philosophy of the Metop radio occultation receiver, the GPSR does not directly output pseudorange and carrier phase observations as expected in common GPS

processing techniques. Instead, the receiver provides a lower-level data set more closely related to the actual tracking process in the receiver. Among others, this includes the code phase as well as the phase of the numerically controlled oscillator (NCO) that is used to remove the residual Doppler shift from the down-converted signal. Traditional pseudorange and carrier phase observations are only generated after data processing on ground. This concept offers a substantially larger flexibility and transparency in the measurement generation, albeit at the expense of a higher operational effort in the ground segment. Among others, different types of receiver time scales can more easily be realized in this approach. A timescale aligned with the estimate of the GPS time determined within the receiver as part of the navigation solution has been used in the present study.

For tracking of the binary phase shift keying (BPSK) modulated L1 C/A signal, a Costas loop with a two-quadrant phase discriminator (Betz 2016) is employed to make the carrier phase tracking independent of the unknown navigation data bits. Depending on the value of the data bit at the start of tracking, the reported NCO phase and the derived carrier phase observation may thus be affected by a constant 180° phase offset over the entire tracking arc. When forming double differences of L1 phase observations across individual tracking channels, half-cycle ambiguities will thus arise. These are of little concern for the POD but detrimental for carrier phase differential GPS navigation.

For tracking the encrypted P(Y) signal, the Swarm GPSR makes use a patented semi-codeless technique (Silvestrin and Cooper 2000) that resembles the well-known Z-tracking (Woo 2000) but uses an improved decision process for estimating the unknown W-bit as well as different assumption for the W-bit duration. The down-converted L1 and L2 signals are first mixed with the output of distinct L1 and L2 NCOs, then correlated with a P-code replica and subsequently integrated over the assumed duration of a W-bit (22 P-code chips). Subject to a positive decision on the W-bit sign, the estimated L1 W-bit is then used to demodulate the P(Y)-code on L2 and vice versa. The W-bit estimation and stripping induces no sign ambiguity and, in principle, enables recovery of the full L2 carrier phase using a four-quadrant discriminator. On the other hand, the processing makes use of the known L1 NCO phase from the L1 C/A code tracking. The L1 half-cycle ambiguities will thus be inherited to the L2 measurements, while the difference of L1 and L2 NCO phases is ensured to be of integer nature. This is consistent with the empirical observation of half-cycle ambiguities in both L1 and L2 phase measurements reported in Allende-Alba and Montenbruck (2016), while WL ambiguities were always found to be integer valued.

The 180° phase shift in the L1 carrier replica that may be caused by the use of a Costas loop results in an associated inversion of the data bits, which can be detected from an inverted preamble (0111010011 instead of 1000101100) and subsequently be used to invert the decoded data stream. Making use of information on the observed sign of the preamble as reported in the raw receiver telemetry, it is possible to correct the reported L1 and L2 NCO phase by 0.5 cycles before forming the carrier phase observations whenever the preamble is inverted. A corresponding modification of the GPSR preprocessing has been developed for this study and used to obtain observation data with full-cycle ambiguities.

Impact of ionospheric scintillation

Starting from the first assessments of GPS data from the Swarm mission, it was possible to observe the impact of ionospheric scintillation on carrier phase observations, whose effects were mostly noticed in polar regions (Sust et al. 2014; Zangerl et al. 2014). Ionospheric scintillation is caused by irregularities in the ionosphere and affects GPS carrier phase observations mainly as diffraction and refraction, originated from the group delay and phase advance as the GPS signal interacts with free electrons along the transmission path (Kintner et al. 2007). It can be considered a form of space-based multipath (Kintner and Ledvina 2005). Further analyses also revealed a performance degradation of the GPS receivers at the equatorial region (Buchert et al. 2015; Xiong et al. 2016).

The temporal and regional dependence of scintillation intensity and its impact on PSOs for Swarm has been extensively analyzed by van den IJssel et al. (2015) and van den IJssel et al. (2016). In comparison with previous analyses, data processed for this study benefit from an improved robustness of the Swarm receivers stemming from the modifications on the carrier tracking loops parameters performed during 2015.

Strategies for space baseline determination

For the first part of this study, precise baselines have been computed using the DLR's GPS High-precision Orbit Determination Software Tools (GHOST; Montenbruck et al. 2005). The reduced-dynamic approach (Yunck et al. 1990; Wu et al. 1991) is applied for POD and PBD schemes, making use of highly precise dynamical models for orbit integration (Montenbruck et al. 2005). Carrier phase integer ambiguities are resolved using a dedicated algorithm based on a batch/sequential estimation of float ambiguities using a priori information from previously computed POD solutions. Subsequently, the solved integer

ambiguities are introduced as known parameters into reduced-dynamic and kinematic baseline determination schemes using single-difference ionosphere-free (IF) observation models. Reduced-dynamic baselines are determined with an extended Kalman filter/smoother. Kinematic solutions are computed using only carrier phase observations with fixed ambiguities (Allende-Alba and Montenbruck 2016). Estimated differential phase variation (PV) maps have been used in the computation of both reduced-dynamic and kinematic baselines. Precise GPS clocks and orbit products have been obtained from the Center for Orbit Determination in Europe (CODE, Dach et al. 2016).

The orbital motion of the Swarm A and Swarm C spacecraft creates a baseline of variable dimension with maximum cross-track separation at the equator of about 160 km (Sieg and Diekmann 2016). This type of long baseline represents a challenging situation for IAR, and consequently for PBD, due to the presence of large ionospheric delays in GPS observations. For the assessment of PBD solutions and the performance of algorithms under such conditions, the present study makes use of a series of inter-product comparisons with solutions from GHOST. Additionally, an inter-agency assessment has been carried out using solutions from the Bernese GNSS Software (BSW, Dach et al. 2015) from the Astronomical Institute of the University of Bern (AIUB).

Results and discussion

PBD solutions have been computed for 90 days of data comprising the period of January to March, 2016. Days January 1 and March 3 have been excluded from the analysis due to the presence of large data gaps or maneuvers. On January 26, roughly half a day of data was not considered in the analysis as a result of anomalous UTC-offset values transmitted by the GPS space segment on that day (Kovach et al. 2016).

Integer ambiguity fixing performance

A major aim of this study is to analyze the performance of IAR algorithms when half-cycle ambiguities are resolved during the generation of carrier phase observations. As an example, Fig. 1 shows the level of improvement on float ambiguity estimation. The plot depicts the frequency distribution of mapped L1 and L2 float ambiguities into the interval [0.5, 1.5] on March 20. As observed, float ambiguity estimates are normally distributed around an integer value. For comparison, a bimodal distribution with peaks at full and half cycles results when processing observations with half-cycle ambiguities. Depending on the observation
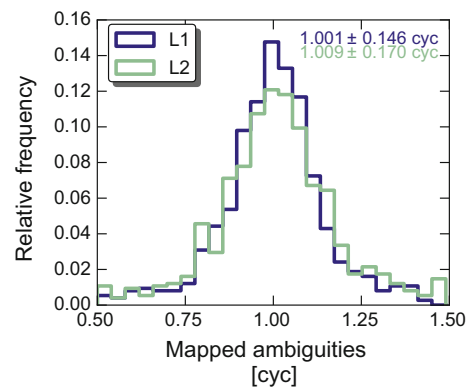

Fig. 1 Frequency distribution of estimated float L1 and L2 ambiguities, mapped into the interval [0.5, 1.5], on March 20, 2016

noise, the distribution modes may, however, be difficult to discern. An almost uniform distribution has in fact been obtained in Allende-Alba and Montenbruck (2016) with such observations.

The representative frequency distribution shown in Fig. 1 provides a rough indication about the expected performance of the IAR scheme: approximately 95% of float ambiguity estimates deviate by less than 0.3 cycles from an integer value and can be fixed with good confidence. Figure 2 shows the integer ambiguity fixing performance for the complete period under analysis. On average, 94% of ambiguities were fixed and used for the computation of reduced-dynamic and kinematic baselines. This value represents an improvement with respect to previous analyses with Swarm data (Jäggi et al. 2014, Allende-Alba and Montenbruck 2016, Mao et al. 2016), where values of 88–89% are reported considering carrier phase observations with half-cycle ambiguities.

Reduced-dynamic baselines

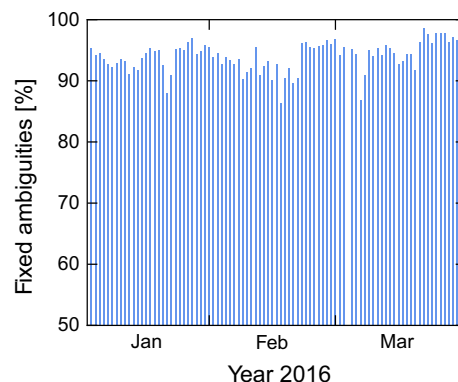An effective assessment of reduced-dynamic baselines is a non-trivial task due to the lack of a reference of any sort.

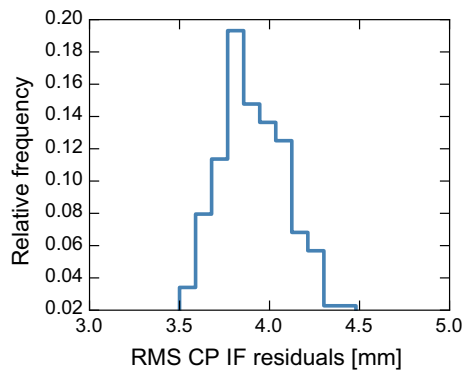**Fig. 2** Carrier phase integer ambiguity fixing performance

Fig. 3 Frequency distribution of daily RMS error of single-difference carrier phase ionosphere-free (CP IF) residuals from reduced-dynamic baseline determination

An initial hint of the baseline quality can be obtained by analyzing the goodness-of-fit of modeled and observed carrier phase measurements using post-fit residuals. Figure 3 depicts the frequency distribution of RMS errors of single-difference carrier phase IF residuals from daily baseline solutions, which provide an indication of the effective receiver carrier phase tracking error levels. As observed, most IF residuals exhibit RMS errors at the level of 3.8–4.1 mm, implying error levels of 1.2–1.3 mm of single-difference observations on individual frequencies.

An external assessment of PBD solutions can be performed by an analysis of satellite laser ranging (SLR, Pearlman et al. 2002) residuals. Such an evaluation provides a tool for a qualitative analysis of the improvement of PBD solutions with respect to their POD counterpart. Figure 4 shows the SLR residuals of normal points from

station Yarragadee, Australia, on February 3 and February 26, 2016, using trajectories from POD and PBD solutions. The SLR station tracks in an alternating way each spacecraft as they pass by the station location. Swarm A's trajectory is used as reference for the computation of PBD solutions, and hence, the residuals are the same for both comparisons. In PBD, the relative trajectory of Swarm C with respect to Swarm A is well constrained by differential pseudorange and carrier phase observations. As seen in Fig. 4 (top), SLR residuals of trajectories from POD solutions appear to be unconnected as they are computed independently. In contrast, Swarm C's trajectory from PBD solutions is more tightly constrained to Swarm A's, as evidenced by the better consistency of SLR residuals for the two spacecraft in Fig. 4 (bottom). Obviously, however, SLR measurement and modeling errors are too large to allow a quantitative assessment of the baseline accuracy at the mm level.

A further evaluation of PBD solutions can be obtained in an inter-product assessment using differential POD (dPOD) solutions, i.e., the difference of individual POD solutions from each spacecraft. This assessment is useful to establish a coarse quality check of baseline products. Figure 5 depicts the comparison of daily dPOD and PBD solutions for the entire period under analysis. On average, RMS errors of 3.3, 7.4 and 4.9 mm could be achieved in the radial, along-track and cross-track directions, respectively. The values obtained are in good accord with similar dPOD-PBD assessments for other formation flying missions such as GRACE (Kroes 2006) and TanDEM-X (Montenbruck et al. 2011).

Fig. 4 SLR residuals of POD (*top*) and PBD (*bottom*) solutions of Swarm A (*blue*) and Swarm C (*red*) at station Yarragadee, Australia, on February 3 (*right*) and February 26 (*left*), 2016, as a function of time. The units are minutes
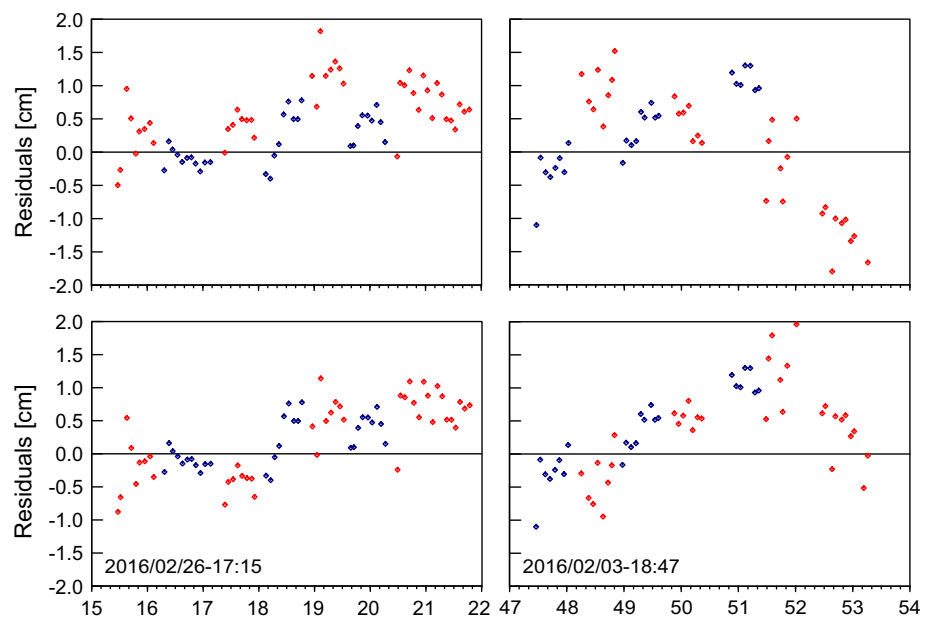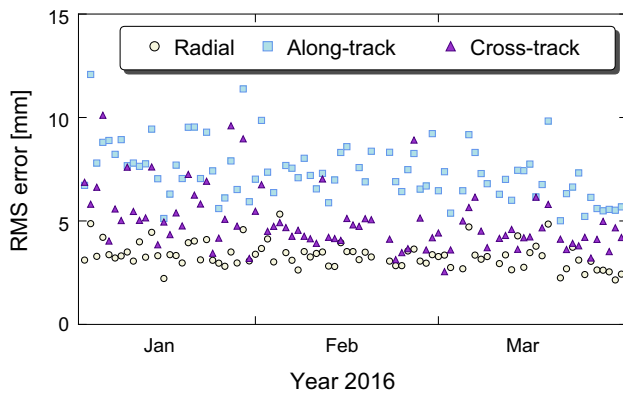
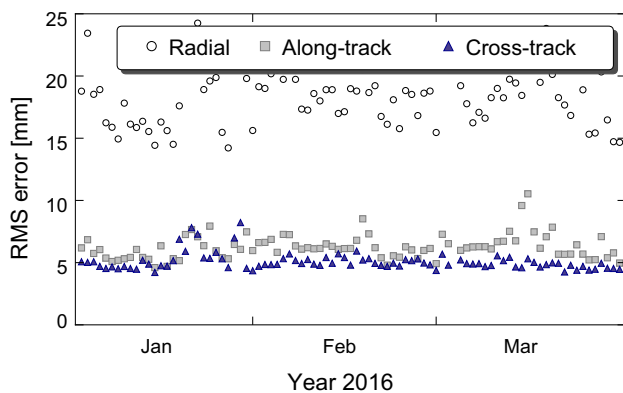**Fig. 5** Daily RMS errors of the difference between dPOD and PBD solutions

Fig. 6 Daily RMS errors of the differences between kinematic and reduced-dynamic baselines

Kinematic baselines

The overall quality of kinematic baselines can be evaluated in comparison with reduced-dynamic solutions. Kinematic solutions are more influenced by the quality of GPS observations and possible wrongly fixed ambiguities, than their reduced-dynamic counterpart. For this assessment, a simple threshold of 50 cm has been selected to discard outlier point solutions stemming from bad data points. The resulting reduction in average number of solutions has been less than 1%. Figure 6 shows the daily RMS errors of the differences between kinematic and reduced-dynamic baseline components. This assessment mainly depicts the effect of the observation geometry and GPS carrier phase effective receiver error levels on the resulting kinematic solutions. In general, there is no apparent variation in time during the period under analysis regarding measurement errors. On average, RMS errors of 18.36, 6.25 and 5.08 mm can be achieved in the radial, along-track and cross-track directions, respectively. In comparison with
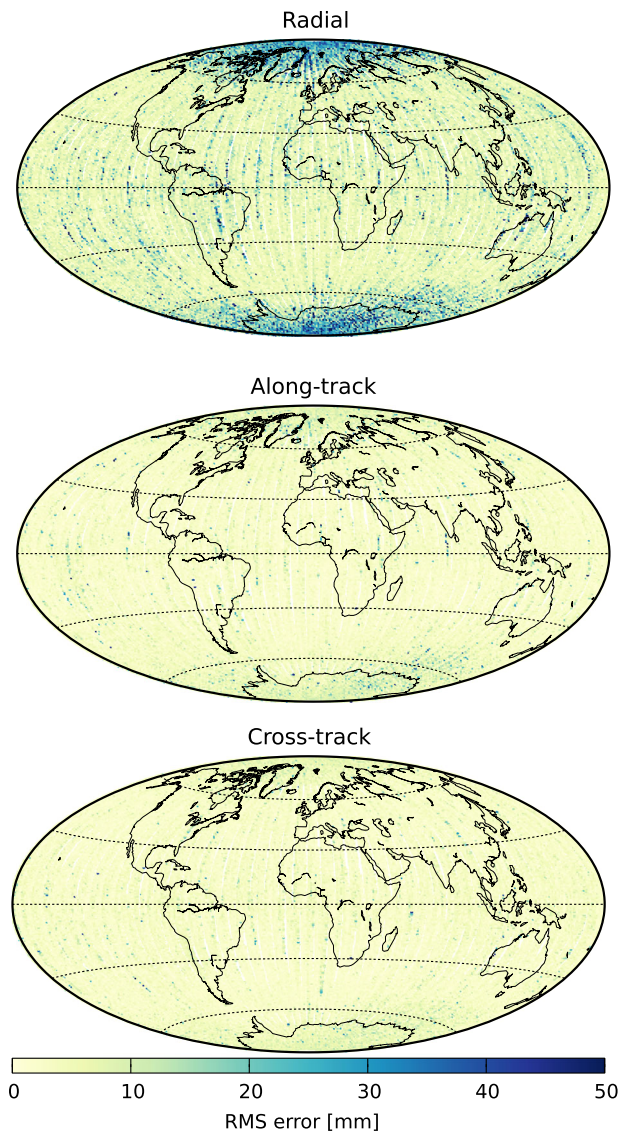

Fig. 7 Global distribution of RMS errors of the differences between kinematic and reduced-dynamic baselines. Swarm A's trajectory has been used for spatial mapping of errors

baseline analyses with data from 2014 (see Jäggi et al. (2014, 2016) and Allende-Alba and Montenbruck (2016)) the obtained error levels mainly suggest an improvement of the ambiguity fixing rate and the quality of carrier phase observations stemming from receiver configuration changes during 2015.

Aside from an analysis in time, an inspection of the spatial distribution of errors in kinematic solutions is useful to observe the geographical dependency of the impact of ionospheric scintillation on carrier phase observations and baseline solutions. Figure 7 shows the global distribution of bin-wise RMS errors of kinematic solutions in each baseline component. As observed, the quality of kinematic baselines is highly affected in the polar regions,

particularly in the radial direction. Solutions over these regions dominate the RMS values derived from Fig. 6. For the radial component, the average RMS errors in the polar regions exceed those in midlatitude regions by a factor of about 2.5, whereas the vertical dilution of precision (VDOP) is, on average, only larger by 0.8. This suggests that the observed solution degradation on latitudes higher than ±60° is mostly caused by increased effective observation error levels due to ionospheric scintillation. Noticeable is the absence of large error signatures that have been observed along the (magnetic) equatorial region in previous POD studies during 2014 (van den IJssel et al. 2015). Although the occurrence and intensity of ionospheric scintillations have a strong dependency on geomagnetic and solar activity, part of the improvement of kinematic solutions may also be attributed to the widening of GPSR carrier tracking loop bandwidths during 2015; see van den IJssel et al. (2016) for a POD analysis in 2015.

Impact of half-cycle ambiguities

When half-cycle ambiguities are present in carrier phase observations, POD solutions are virtually not affected, with changes at the 0.1 mm level in dPOD solutions. However, baseline solutions from standard IAR/PBD schemes may be degraded if no adaptation or tailoring strategies are applied. A comparison of baseline solutions using different approaches can be evaluated to observe the impact of half-cycle ambiguities in PBD. For this test, kinematic baselines are computed using all available carrier phase observations with float and fixed ambiguities. Reduced-dynamic baseline solutions are used as reference for assessment.

If half-cycle ambiguities are not resolved during pre-processing of GPSR data, the PBD algorithm has to cope with carrier phase observations with the same statistical distribution of half- and full-cycle ambiguities. Figure 8 (top and middle) shows an example assessment of kinematic baselines in the along-track direction on February 29. The solutions are computed using the methods developed in Allende-Alba and Montenbruck (2016), denoted as "half-cycle" and "mixed-cycle" IAR schemes. As observed, by taking into account such adaptation techniques, it is possible to obtain baselines with reasonable quality, at the expense of an increased complexity in the processing algorithms. During this day, the obtained ambiguity fixing rates for each scheme are 92 and 95%, respectively. Figure 8 (bottom) shows the corresponding assessment of a solution computed using carrier phase observations with full-cycle ambiguities only. The achieved ambiguity fixing rate with this approach is of 97%.

Apart from a slight overall improvement of kinematic solutions provided by carrier phase observations with full-cycle ambiguities, a further benefit lies in the performance of IAR/PBD algorithms. In particular, the scheme denoted as "mixed-cycle" IAR requires a 2–2.5× increase in processing time in comparison with an IAR processing of full-cycle ambiguities only. This suggests that the strategy presented in this study allows an overall improvement of the performance of standard IAR/PBD schemes and quality of baseline solutions without requiring any adaptation or special consideration in the processing algorithms.

Fig. 8 Assessment of kinematic baselines on February 29. Solutions shown in *top* and *middle* plots have been computed using uncorrected (with half-cycle ambiguities) observation files, employing the "half-cycle" and "mixed-cycle" IAR approaches, respectively. The solution shown in the *bottom plot* has been computed using carrier phase observations with full-cycle ambiguities only
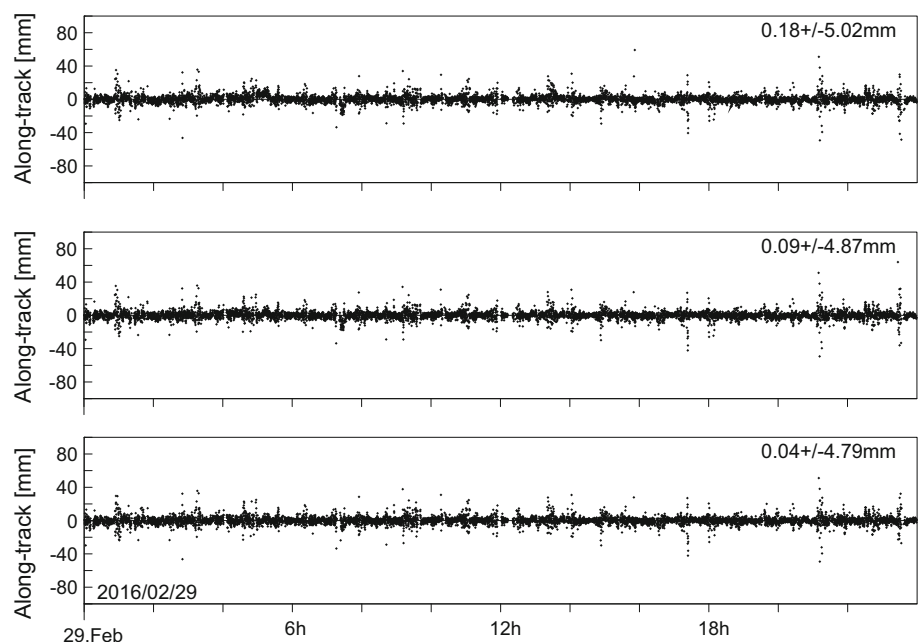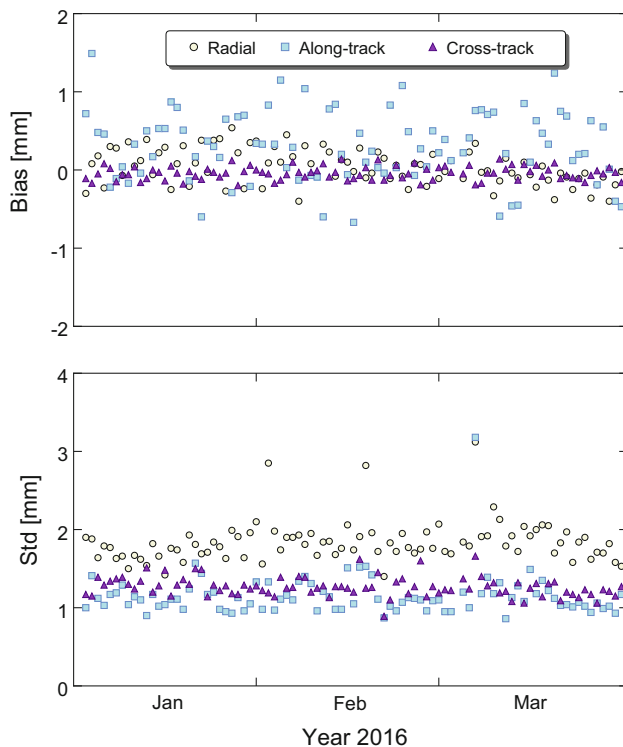
Fig. 9 Comparison of daily reduced-dynamic baseline solutions from GHOST and BSW

Table 1 Average values of reduced-dynamic and kinematic baseline comparison using solutions from GHOST and BSW

Component	Reduced-dynamic (mm)		Kinematic (mm)	
	Bias	Std	Bias	Std
Radial	0.03	1.83	0.53	17.17
Along-track	0.29	1.15	−0.32	5.83
Cross-track	−0.04	1.26	0.10	5.07
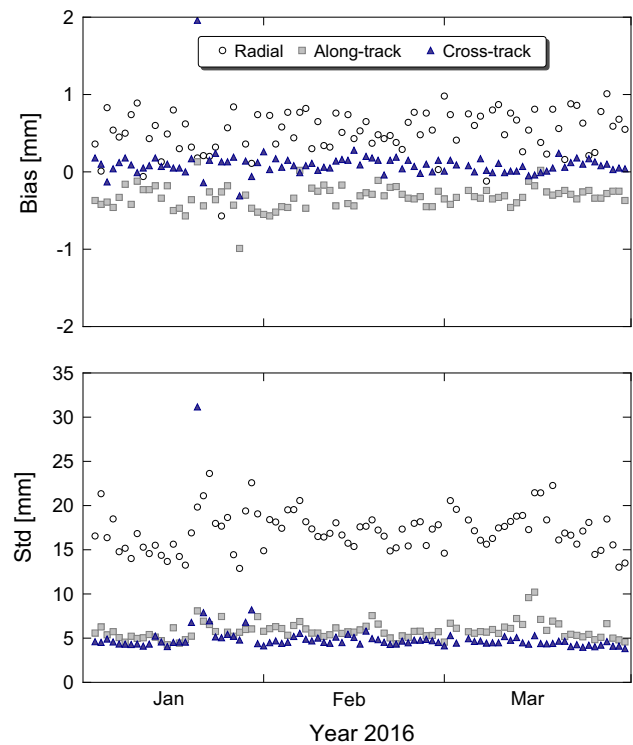
Fig. 10 Comparison of daily kinematic baseline solutions from GHOST and BSW

Inter-agency baseline comparison

Baselines from the GHOST software have been further assessed using external and independent solutions computed using the BSW at AIUB. In BSW, reduced-dynamic and kinematic solutions are computed using a batch least-squares estimation scheme using double-difference IF GPS observations with fixed carrier phase integer ambiguities, resolved using the WL/NL approach. See Jäggi et al. (2007) for details.

The comparison of reduced-dynamic baselines is shown in Fig. 9. Table 1 depicts the resulting average values of the comparison. In this assessment, some hours during days 50, 51 and 79 have been excluded due to the presence of large data gaps. As observed in Fig. 9 (top), the biases among solutions are well confined below 1 mm, providing an indication of low systematic errors in the solutions. Additionally, regarding average standard deviation [Table 1; Fig. 9 (bottom)], the achieved consistency of solutions lies in the 1–2 mm range. In comparison with similar assessments using data from the GRACE and TanDEM-X missions (Jäggi et al. 2009b, 2012), reduced-dynamic baseline solutions from Swarm appear to be slightly degraded. This may be attributed mainly to both the larger carrier phase errors in the observations and the

reduced number of available tracking channels in the GPSR instruments.

Similar to the assessment shown in Fig. 6, for the comparison of kinematic baselines from GHOST and BSW, a simple threshold has been used to discard outlier solutions. Figure 10 shows the resulting comparison. As in the case of reduced-dynamic solutions, most of the biases of kinematic baselines are below 1 mm [Fig. 10 (top)]. However, a relatively large average bias in the radial direction between both kinematic solution types is present (Table 1). The main cause for this is still under investigation. The consistency of solutions shown in Fig. 10 (bottom) is in good agreement with the values obtained in the inter-product assessment of GHOST solutions (Fig. 6). On average, standard deviations are obtained in the range

of 5–6 mm for the horizontal components and around 17 mm in the radial direction, as shown in Table 1.

Conclusions

The present study has shown the feasibility of generating carrier phase observations with full-cycle ambiguities from the GPSR receivers onboard the Swarm spacecraft. The resulting observation files have helped to improve the performance of IAR, reduced-dynamic and kinematic baseline determination schemes. Precise baseline products have been computed using the GHOST software, and they have been assessed using inter-product and inter-agency comparisons. The results show an average integer ambiguity fixing rate of around 94%. A consistency of reduced-dynamic baselines and dPOD solutions of better than 1 cm (3D RMS) has been achieved. Average errors of kinematic baselines of around 5–6 and 18 mm have been achieved in the horizontal and vertical components, respectively. The inter-agency assessment using solutions from the AIUB's BSW shows a consistency of reduced-dynamic baselines at the level of 1–2 mm (3D RMS). Similarly, kinematic baselines are consistent at the 5 and 17 mm level in the horizontal and vertical components, respectively. Altogether, these results suggest the feasibility of generating precise reduced-dynamic and kinematic baselines for the Swarm mission, being of particular interest for applications on earth system monitoring and gravity field determination.

References

Allende-Alba G, Montenbruck O (2016) Robust and precise baseline determination of distributed spacecraft in LEO. Adv Space Res 57(1):46–63. doi:10.1016/j.asr.2015.09.034

Betz J (2016) Engineering satellite-based navigation and timing—global navigation satellite systems, signals, and receivers. Wiley-IEEE Press, Hoboken

Bock H, Jäggi A, Meyer U, Visser P, van den IJssel J, van Helleputte T, Heinze M, Hugentobler U (2011) GPS-derived orbits for the GOCE satellite. J Geodesy 85(11):807–818

Buchert S, Zangerl F, Sust M, André M, Eriksson A, Wahlund JE, Opgenoorth H (2015) SWARM observations of equatorial electron densities and topside GPS track losses. Geophys Res Lett 42(7):2008–2092. doi:10.1002/2015GL063121

Dach R, Lutz S, Walser P, Fridez P (eds) (2015) Bernese GNSS Software version 5.2. User manual. Astronomical Institute, University of Bern, Bern Open Publishing. doi:10.7892/boris.72297

Dach R, Schaer S, Arnold D, Orliac E, Prange L, Sušnik A, Villiger A, Jäggi A (2016) CODE final product series for the IGS. Published by Astronomical Institute, University of Bern. doi:10.7892/boris.75876

Flechtner F, Morton P, Watkins P, Webb F (2014) Status of the GRACE Follow-on mission. In: Gravity, geoid and height systems, IAG symposia, vol. 141. pp 117-121. doi:10.1007/978-3-319-10837-715

Friis-Christensen E, Lühr H, Hulot G (2006) Swarm: a constellation to study the Earth's magnetic field. Earth Planets Space 58(4):351–358. doi:10.1186/BF03351933

Friis-Christensen E, Lühr H, Knudsen D, Haagmans R (2008) Swarm—an earth observation mission investigating geospace. Adv Space Res 41(1):210–216. doi:10.1016/j.asr.2006.10.008

Gerlach C, Visser PNAM (2006) SWARM and gravity: possibilities and expectations for gravity field recovery. In: Proceedings of the first international science meeting, SWARM, ESA WPP-261

Jäggi A, Hugentobler U, Bock H, Beutler G (2007) Precise orbit determination for GRACE using undifferenced or doubly differenced GPS data. Adv Space Res 39(10):1612–1619. doi:10.1016/j.asr.2007.03.012

Jäggi A, Beutler G, Prange L, Dach R (2009a) Assessment of GPS-only observables for gravity field recovery from GRACE. In: Sideris MG (ed) Observing our changing earth. IAG symposia, vol. 33. pp 113–123. doi:10.1007/978-3-540-85426-514

Jäggi A, Dach R, Montenbruck O, Hugentobler U, Bock H, Beutler G (2009b) Phase center modeling for LEO GPS receiver antennas and its impact on precise orbit determination. J Geodesy 83:1145–1162. doi:10.1007/s00190-009-0333-2

Jäggi A, Montenbruck O, Moon Y, Wermuth M, König R, Michalak G, Bock H, Bodenmann D (2012) Inter-agency comparison of TanDEM-X baseline solutions. Adv Space Res 50(2):260–271. doi:10.1016/j.asr.2012.03.027

Jäggi A, Dahle C, Arnold D, Meyer U, Bock H (2014) Kinematic space-baselines and their use for gravity field recovery. Presented at the 40th COSPAR Scientific Assembly, Moscow, Russia, Aug 2014. doi:10.7892/boris.58970

Jäggi A, Dahle C, Arnold D, Bock H, Meyer U, Beutler G, van den IJssel J (2016) Swarm kinematic orbits and gravity fields from 18 months of GPS data. Adv Space Res 57(1):218–233. doi:10.1016/j.asr.2015.10.035

Kintner PM, Ledvina BM (2005) The ionosphere, radio navigation, and global navigation satellite systems. Adv Space Res 35(5):788–811. doi:10.1016/j.asr.2004.12.076

Kintner PM, Ledvina BM, de Paula ER (2007) GPS and ionospheric scintillations. Space Weather 5:S09003

Kovach K, Mendicki PJ, Powers E, Renfro B (2016) GPS receiver impact from the UTC Offset (UTCO) Anomaly of 25–26 Jan 2016. In: Proceedings of ION GNSS+, Institute of Navigation, Portland, Oregon, Sept 12–13, pp 2887–2895

Krieger G, Hajnsek I, Papathanassiou KP, Younis M, Moreira A (2010) Interferometric synthetic aperture radar (SAR) missions employing formation flying. Proc IEEE 98(5):816–843

Kroes R (2006) Precise relative positioning of formation flying spacecraft using GPS. Ph.D. thesis, TU Delft

Mackenzie R, Bock R, Kuijper D, Ramos-Bosch P, Sieg D, Ziegler G (2014) A review of Swarm flight dynamics operations from launch to routine phase. In: Proceedings of the 24th international symposium on space flight dynamics, May 2014

Mao X, Visser PNAM, van den IJssel J, Doornbos E (2016) Swarm absolute and relative orbit determination. Presented at: living planet symposium, ESA SP-740, May 2016. http://lps16.esa.int/

posterfiles/paper1458/ID1458_Mao_Swarm Orbit Determination.pdf

Montenbruck O, van Hellepute T, Kroes R, Gill E (2005) Reduced-dynamic orbit determination using GPS code and carrier measurements. Aerosp Sci Technol 9(3):261–271. doi:10.1016/j.ast.2005.01.003

Montenbruck O, Andres Y, Bock H, van Helleputte T, van den IJssel J, Loiselet M, Marquardt C, Silvestrin P, Visser P, Yoon Y (2008) Tracking and orbit determination performance of the GRAS instrument on MetOp-A. GPS Solut 12(4):289–299. doi:10.1007/s10291-008-0091-2

Montenbruck O, Wermuth M, Kahle R (2011–2012) GPS based relative navigation for the TanDEM-X mission—first flight results. Navigation, 58(4):293–304. doi: 10.1002/j.2161-4296.2011.tb02587.x

Pearlman MR, Degnan JJ, Bosworth JM (2002) The international laser ranging service. Adv Space Res 30(2):135–143. doi:10.1016/S0273-1177(02)00277-6

Reigber Ch, Lühr H, Schwintzer P (2002) CHAMP mission status. Adv Space Res 30(2):129–134. doi:10.1016/S0273-1177(02)00276-4

Sieg D, Diekmann FJ (2016) Options for the further orbit evolution of the Swarm mission. In: Proceedings of the living planet symposium, ESA SP-740, August

Silvestrin P, Cooper J (2000) Method of processing of signals of a satellite positioning system. US Patent 6 157 341, Dec 5

Silvestrin P, Bagge P, Bonnedal M, Carlstrom A, Christensen J, Hagg M, Lindgren T, Zangerl F (2000) Spaceborne GNSS radio occultation instrumentation for operational applications. In: Proceedings ION GPS, Institute of Navigation, Salt Lake City, UT, Sept 19–22, pp 872–880

Sust M, Zangerl F, Montenbruck O, Buchert S, Garcia-Rodriguez A (2014) Spaceborne GNSS receiving system performance prediction and validation. In: NAVITEC: ESA workshop on satellite navigation technologies and GNSS Signals and signal processing

Tapley BD, Bettadpur S, Watkins M, Reigber C (2004) The gravity recovery and climate experiment: mission overview and early results. Geophys Res Lett. doi:10.1029/2004GL019920

Teixeira da Encarnação J, Arnold D, Bezděk A, Dahle C, Doornbos E, van den IJssel J, Jäggi A, Mayer-Gürr T, Sebera J, Visser PNAM, Zehentner N (2016) Gravity field models derived from Swarm GPS data. Earth Planets Space 68:27

van den IJssel J, Encarnação J, Doornbos E, Visser P (2015) Precise science orbits for the Swarm satellite constellation. Adv Space Res 56(6):1042–1055. doi:10.1016/j.asr.2015.06.002

van den IJssel J, Forte B, Montenbruck O (2016) Impact of swarm GPS receiver updates on POD performance. Earth Planets Space 68(1):1–17. doi:10.1186/s40623-016-0459-4

Wang X, Rummel R (2012) Using Swarm for gravity field recovery: first simulation results. In: Sneeuw N, Novák P, Crespi M, Sansò F (eds) VII Hotine-Marussi symposium on mathematical geodesy, IAG Symposia, vol. 137, pp 301–306. doi: 10.1007/978-3-642-22078-4 45

Woo KT (2000) Optimum semi-codeless carrier phase tracking of L2. Navigation 47(2):82

Wu SC, Yunck TP, Thornton CL (1991) Reduced-dynamic technique for precise orbit determination of low Earth satellites. J Guid Control Dyn 14(1):24–31

Xiong C, Stolle C, Lühr H (2016) The Swarm satellite loss of GPS signal and its relation to ionospheric plasma irregularities. Space Weather 14(8):563–577. doi:10.1002/2016SW001439

Yunck TP, Wu SC, Wu JT, Thornton CL (1990) Tracking of remote satellites with the global positioning system. IEEE Trans Geosci Remote Sens 28(1):108–116

Zangerl F, Griesauer F, Sust M, Montenbruck O, Buchert B, Garcia A (2014) SWARM GPS precise orbit determination receiver initial in orbit performance evaluation. In: Proceedings ION GNSS+, Institute of Navigation, Tampa, Florida, Sept 8–12, pp 1459–1468

Zin A, Landenna S, Conti A (2006) Satellite-to-satellite tracking instrument—design and performance. Presented at the 3rd international GOCE user workshop, Nov 6–8 Nov 2006, ESA-ESRIN, Frascati, Italy

Gerardo Allende-Alba is a Ph.D. candidate at the Technische Universität München and the DLR's German Space Operations Center. In 2012 he received his M.Sc. in earth-oriented space science and technology from the Technische Universität München and his B.Sc. in 2008 from the Instituto Politécnico Nacional in Mexico. His current research activities are focused on precise orbit and space baseline determination using GNSS carrier phase observations.

Oliver Montenbruck is head of the GNSS Technology and Navigation Group at DLR's German Space Operations Center. His research activities comprise spaceborne GNSS receiver technology, autonomous navigation systems, spacecraft formation flying and precise orbit determination as well as new constellations and multi-GNSS processing. Oliver Montenbruck presently chairs the Multi-GNSS Working Group of the International GNSS Service and coordinates the performance of the MGEX Multi-GNSS Experiment.

Adrian Jäggi is a professor of the Phil.-nat.-Faculty of the University of Bern and director of the Astronomical Institute. In 2006 he received his Ph.D. in astronomy from the University of Bern, and in 2007 he became Carl von Linde Junior Fellow at the Institute for Advanced Study of the Technische Universität München. His main research activities comprise precise orbit determination and global gravity field recovery using low earth satellites and GNSS.

Daniel Arnold is a senior researcher at the Astronomical Institute of the University of Bern. He is responsible for LEO orbit and gravity field determination at AIUB and in charge of the routine processing of GNSS orbits and clocks for the CODE analysis center. Since January 2016 he is the head of the satellite geodesy subgroup LEO orbit and gravity field determination.

Franz Zangerl received his M.Sc. in electrical engineering from the Technische Universität Wien in 1990. He is the leader of the processing system group at RUAG Aerospace Austria. Since 1997 he is working as a system engineer in the area of GNSS receivers for space applications.